The Company of **Biologists**

RESEARCH ARTICLE

Tbx6, Mesp-b and Ripply1 regulate the onset of skeletal myogenesis in zebrafish

Stefanie E. Windner[1], Rosemarie A. Doris[1,*], Chantal M. Ferguson[1,*], Andrew C. Nelson[2,*], Guillaume Valentin[3,*], Haihan Tan[2], Andrew C. Oates[3], Fiona C. Wardle[2] and Stephen H. Devoto[1,‡]

ABSTRACT

During embryonic development, the paraxial mesoderm becomes segmented into somites, within which proliferative muscle progenitors and muscle fibers establish the skeletal musculature. Here, we demonstrate that a gene network previously implicated in somite boundary formation, involving the transcriptional regulators Tbx6, Mesp-b and Ripply1, also confers spatial and temporal regulation to skeletal myogenesis in zebrafish. We show that Tbx6 directly regulates *mesp-b* and *ripply1* expression *in vivo*, and that the interactions within the regulatory network are largely conserved among vertebrates. Mesp-b is necessary and sufficient for the specification of a subpopulation of muscle progenitors, the central proportion of the Pax3^{+}/Pax7^{+} dermomyotome. Conditional ubiquitous expression indicates that Mesp-b acts by inhibiting myogenic differentiation and by inducing the dermomyotome marker *meox1*. By contrast, Ripply1 induces a negative-feedback loop by promoting Tbx6 protein degradation. Persistent Tbx6 expression in Ripply1 knockdown embryos correlates with a deficit in dermomyotome and myotome marker gene expression, suggesting that Ripply1 promotes myogenesis by terminating Tbx6-dependent inhibition of myogenic maturation. Together, our data suggest that Mesp-b is an intrinsic upstream regulator of skeletal muscle progenitors and that, in zebrafish, the genes regulating somite boundary formation also regulate the development of the dermomyotome in the anterior somite compartment.

INTRODUCTION

Skeletal musculature in the vertebrate embryo originates in the paraxial mesoderm, which develops on either side of the neural tube and notochord, and subsequently segments into somites. Segmentation of paraxial mesoderm into somites and myogenesis within each somite are sequentially initiated, starting posterior to the head and progressing towards the tail bud, which simultaneously produces more paraxial mesoderm to elongate the body axis (Buckingham and Vincent, 2009; Oates et al., 2012). How the onset of myogenesis is coordinated with the formation of somites is not yet understood.

[1]Department of Biology, Wesleyan University, Middletown, CT 06459, USA. [2]Randall Division of Cell and Molecular Biophysics, New Hunt's House, King's College London, Guy's Campus, London, SE1 1UL, UK. [3]MRC National Institute for Medical Research, The Ridgeway, Mill Hill, London, NW7 1AA, UK.
*These authors contributed equally to this work

‡Author for correspondence (sdevoto@wesleyan.edu)

Expression of the paired domain transcription factor *pax3* marks the entry of paraxial mesoderm cells into the myogenic program before their incorporation into a somite (Kusakabe and Kuratani, 2005; Buckingham and Relaix, 2007). Subsequently, Pax3-expressing cells give rise to two spatially segregated myogenic tissues. The dermomyotome, a transient epithelial structure containing proliferative muscle progenitors, is located at the lateral somite surface; the myotome, consisting of differentiated muscle fibers, lies underneath/medial to the dermomyotome. Muscle progenitors retain *pax3* expression and upregulate *pax7*, whereas differentiating muscle fibers downregulate *pax3* and express myogenic regulatory factors like *myoD* and *myf5* (Buckingham and Rigby, 2014).

The zebrafish myotome consists of spatially segregated slow and fast muscle fibers, which are specified in the pre-somitic paraxial mesoderm. First, Hedgehog signaling from the notochord and ventral neural tube induces slow muscle fibers in the adjacent medial paraxial mesoderm (Blagden et al., 1997; Du et al., 1997). Then, immediately before somite boundary formation, Hedgehog and Fgf8 signaling promote differentiation of fast fibers in the *pax3*-expressing lateral paraxial mesoderm, specifically in the posterior half of the future somite (Groves et al., 2005; Hammond et al., 2007). After somite formation, *pax3*-expressing cells in the anterior half of the lateral somite upregulate *pax7* and translocate to the surface of the developing myotome (Hollway et al., 2007; Stellabotte et al., 2007). It is unknown how the onset of *myoD* expression becomes restricted to the posterior half of the lateral somite. Similarly, it is unknown what promotes the development of Pax3^{+}/Pax7^{+} dermomyotome cells in the anterior half of the lateral somite.

The establishment of anterior and posterior half-somite domains has been studied in the context of segmentation, because the polarized/alternating expression of genes in the pre-somitic mesoderm precedes somite boundary formation (Dahmann et al., 2011). The patterning process begins in the tailbud, where single cells initiate oscillating expression of members of the Her/Hes family of bHLH transcriptional repressors, which are subsequently synchronized among neighboring cells by Delta-Notch signaling (Pourquié, 2011; Oates et al., 2012). Before morphological boundary formation, these oscillations, known as the segmentation clock, are translated into non-oscillating expression of genes specific to either prospective anterior or posterior half-somites (Saga, 2012).

tbx6/fused somites encodes a T-box transcription factor required for the maintenance and readout of these oscillations in the anterior pre-somitic mesoderm, and for the formation of somite boundaries in zebrafish (van Eeden et al., 1996; Nikaido et al., 2002; Oates et al., 2005; Brend and Holley, 2009). We recently discovered that Tbx6 is also required for the development of a subpopulation of dermomyotome cells (Windner et al., 2012). *tbx6* mutants

ectopically upregulate *myoD* in the anterior half-somite, which correlates with a gain in fast fiber nuclei and a loss of the central domain of the Pax3$^+$/Pax7$^+$ dermomyotome, whereas peripheral (dorsal and ventral) dermomyotome develops normally. These findings suggest that Tbx6 inhibits premature differentiation of dermomyotome cells, and provide an unexpected link between myogenesis and somite boundary formation.

In mouse, expression of the bHLH transcription factor *Mesp2* is induced by the combination of Tbx6 and spatially restricted Notch signaling, specifically in the anterior half of the future somite (Yasuhiko et al., 2006). Mesp2 promotes morphological somite boundary formation via activation of Eph/Ephrin signaling and activates co-repressors of the Ripply family, which terminate the patterning network by negatively regulating Tbx6 function (Nakajima et al., 2006; Takahashi et al., 2010). *mesp* and *ripply* genes are expressed in a Tbx6-dependent manner and also regulate anterior-posterior somite polarity in zebrafish (Sawada et al., 2000; Kawamura et al., 2005); however, it is unknown whether they play a role in myogenesis.

Here, we analyze the Tbx6–Mesp-b–Ripply1 regulatory network in zebrafish and reveal its role at the onset of skeletal myogenesis. We show that both *mesp-b* paralogs and *ripply1* are direct targets of Tbx6. Mesp-b is necessary and sufficient for development of the central domain of the Pax3$^+$/Pax7$^+$ dermomyotome, similar to Tbx6. Mesp-b inhibits *myoD* and *myf5* expression, and by inducing the dermomyotome marker *meox1* in the anterior half of future somites. By contrast, Ripply1 negatively regulates *mesp-b* expression by eliminating Tbx6 protein. This negative-feedback loop, which is also promoted by Mesp-b, is required for upregulation of *pax3/7* as well as *myoD* and *myf5*, suggesting a Tbx6-dependent inhibition of myogenic gene expression. Our results provide an explanation for the spatially restricted development of myogenic progenitors within the somites, and for the temporal coordination of myogenesis with the formation of somite boundaries.

RESULTS
Tbx6 directly regulates *mesp-b* and *ripply1* expression

Tbx6 is required for the expression of *mesp-b* and *ripply1* in the paraxial mesoderm during somite formation, and for the specification of the central Pax3$^+$/Pax7$^+$ dermomyotome (Sawada et al., 2000; Kawamura et al., 2005; Windner et al., 2012). At the 10-somite stage (14 h post fertilization), *tbx6* mRNA was highly expressed throughout the anterior pre-somitic mesoderm, and at decreasing levels in the recently formed somites SI-SIII, whereas, surprisingly, Tbx6 protein was downregulated prior to somite formation (Fig. 1A,B). Specifically, Tbx6 protein was reduced in the posterior proportion of S-I and virtually undetectable throughout the S-0 domain (antibody specificity shown in supplementary material Fig. S1). *mesp-ba* and *ripply1* mRNA spatially overlapped with Tbx6 protein (Fig. 1C,D): *mesp-ba* was expressed in two precise stripes in the future anterior half-somite in S-II and S-I; *ripply1* expression was initiated in the future posterior half-somite in S-I, highly upregulated throughout the anterior and posterior of S-0 and SI, and gradually downregulated and restricted to the anterior half in the maturing somites. *myoD* was co-expressed with Tbx6 in the developing slow muscle fibers along the medial somite surface, but did not overlap with Tbx6 in the lateral paraxial mesoderm (Fig. 1E).

We carried out chromatin immunoprecipitation, followed by high throughput sequencing (ChIP-seq) of DNA associated with Tbx6. Because the Tbx6 antibody did not work for ChIP (data not shown),

we used a transgenic zebrafish line with heat shock-inducible Myc-tagged Tbx6, *Tg(hsp70l:tbx6^{myc})^{v8}*, that can rescue the *tbx6* mutant phenotype (Windner et al., 2012), and immunoprecipitated with an anti-Myc antibody 1 h after transgene induction. We identified regions of Tbx6 binding in close proximity to the *mesp-ba*, *mesp-bb* and *ripply1* genes (Fig. 1F; supplementary material Table S1), many of which match those found computationally using the T-box consensus motif (Cutty et al., 2012). *De novo* motif discovery showed that the Tbx6^{Myc} *in vivo* binding sequences included the consensus T-box previously identified for T-box proteins in zebrafish and mouse (Kispert and Hermann, 1993; Garnett et al., 2009) (Fig. 1G; supplementary material Table S2). The binding site near the transcriptional start site of *mesp-ba* has been confirmed previously by Kawamura et al. (2008); we confirmed the binding site ~6700 bp upstream of the transcription start site by ChIP-PCR (supplementary material Fig. S2).

Combined, these data suggest that Tbx6 directly regulates the *mesp-b* and *ripply1* genes *in vivo*. The expression of *mesp-b* and *ripply1* precedes the development of dermomyotome cells in the anterior half-somite and fast muscle fibers in the posterior half-somite (Fig. 1H).

Mesp-b is necessary and sufficient for central dermomyotome formation

To test whether *mesp-b* regulates dermomyotome development in the anterior half-somite, we knocked down Mesp-b function using morpholinos (MOs) against both zebrafish paralogs (Mesp-ba and Mesp-bb MOs, henceforth referred to as Mesp-b MO). Knockdown of either Mesp-ba or Mesp-bb alone did not result in a dermomyotome phenotype (data not shown), suggesting functional redundancy between *mesp-b* paralogs. We found that translation-blocking and splice-blocking Mesp-b MOs produced similar phenotypes, and validated the functionality of the splice-blockers by RT-PCR (supplementary material Fig. S3). As previously reported, *ripply1* mRNA was expressed in the pre-somitic mesoderm in Mesp-b morphants; however, expression was not maintained after somite boundary formation (Kawamura et al., 2005) (Fig. 2A).

The dermomyotome marker *meox1* and the myotome marker *myoD* were similarly expressed in pre-somitic mesoderm in control and Mesp-b MO-injected embryos, but showed complementary changes within the somites: in newly formed somites, *meox1* was reduced and *myoD* expanded to the anterior half-somite, whereas in more mature somites, neither mRNA was maintained in the lateral somite (Fig. 2B,C). *myoD* expression in slow muscle progenitors along the medial somite surface was not affected in Mesp-b morphants. The transient upregulation of *myoD* in anterior and posterior half-somites resembled the pattern of *myoD* expression in *tbx6* mutants (van Eeden et al., 1996; Windner et al., 2012), and, together with a downregulation of *meox1*, suggests a loss of dermomyotome and an expansion of fast muscle development.

Indeed, the number of Pax7$^+$ dermomyotome cells was reduced in Mesp-b morphants, specifically in the central domain of the trunk, identical to the dermomyotome phenotype in *tbx6* mutants at the 24-h stage (Fig. 2D-F). The loss of central, but not peripheral, dermomyotome in *tbx6* mutant and Mesp-b knockdown embryos was consistent with the restriction of *mesp-b* expression to the central proportion of the paraxial mesoderm (supplementary material Fig. S4). We conclude that, downstream of Tbx6, Mesp-b is required for central dermomyotome development.

To test whether Mesp-b can rescue central dermomyotome development in the absence of *tbx6*, we created transgenic fish
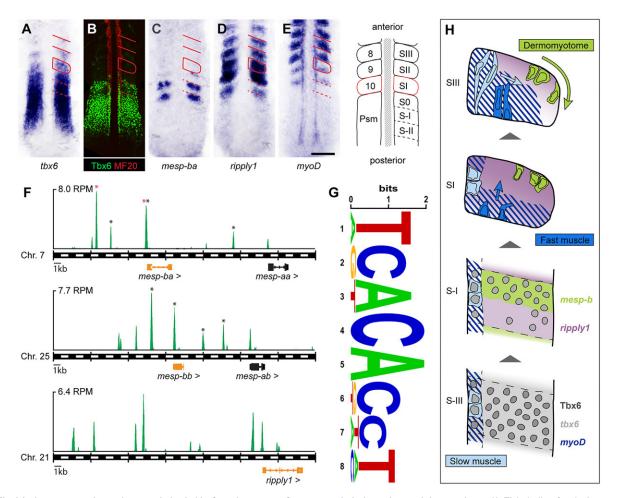
Fig. 1. Tbx6 induces *mesp-b* paralogs and *ripply1* before the onset of myogenesis in lateral paraxial mesoderm. (A-E) Labeling for *tbx6*, *mesp-ba*, *ripply1* and *myoD* mRNAs, and for Tbx6 and myosin heavy chain (MF20) proteins at the 10-somite stage. Unbroken lines indicate most recently formed somites (SI-SIII); dashed lines indicate future somites (S0, S-I, S-II) in the anterior pre-somitic mesoderm (PSM). Scale bar: 100 μm. (F) Anti-Myc immunoprecipitation from *Tg(hsp70l:tbx6^{myc})* embryos 1 h after heat shock and subsequent sequencing reveals Tbx6^{Myc} genomic binding proximal to *mesp-ba*, *mesp-bb* and *ripply1*. Shown are 35-kb windows encompassing significant peaks in reads per million (RPM) (supplementary material Table S1). Black asterisks indicate correspondence with T-box binding sites identified by Cutty et al. (2012). Red asterisks indicate peaks confirmed by ChIP-PCR (supplementary material Fig. S2). (G) Top sequence motif found in Tbx6^{Myc} binding peaks (supplementary material Table S2). (H) Schematic showing spatial and temporal correlation of *tbx6*, *mesp-ba* and *ripply1* expression with the onset of dermomyotome and myotome (slow and fast fiber) development (adapted from Stellabotte and Devoto, 2007).

with a heat shock-inducible promoter driving ubiquitous expression of Myc-tagged Mesp-ba, *Tg(hsp70l:mesp-ba^{myc})*. Transgene expression in *tbx6* mutants during segmentation stages caused an increase in the number of Pax7+ central dermomyotome cells at the 24-h stage, and rescued medio-lateral patterning of slow and fast muscle fibers, which is disrupted in *tbx6* mutants (Fig. 2G-K). At the 36-h stage, the number of Pax7+ dermomyotome cells and the size of the myotome in transgenic *tbx6* mutants were increased when compared with non-transgenic siblings, and resembled those in wild-type embryos (Fig. 2L-N). Thus, ubiquitous Mesp-ba expression is sufficient to rescue myogenic phenotypes found in *tbx6* mutants (Windner et al., 2012).

tbx6 mutants do not form somite boundaries (*fused somites* phenotype) (van Eeden et al., 1996). By contrast, Mesp-b morphants formed irregular somites (Fig. 2A-C) and showed clearly segmented myotomes, as indicated by expression of the myogenic enhancer factor Mef2 and myosin heavy chain protein (MF20) in differentiated muscle fibers (Fig. 2D-F). Conversely, ubiquitous Mesp-ba expression did not fully rescue somite boundary formation in *tbx6* mutants, but resulted in the

formation of partial and irregularly spaced myotome boundaries (Fig. 2M).

Combined, these knockdown and rescue experiments suggest that Mesp-b is necessary and sufficient for central dermomyotome development downstream of Tbx6, but not necessary/sufficient for somite boundary formation.

Mesp-b inhibits myogenic differentiation and promotes dermomyotome development

To further examine the role of Mesp-b in central dermomyotome development, we analyzed the immediate effects of ubiquitous Mesp-ba^{Myc} expression on genes characterizing the onset of dermomyotome development (*meox1*, *pax3*) and myogenic differentiation (*myoD*, *myf5*) in wild-type embryos. Transient overexpression of Mesp-ba led to the opposite effect of Mesp-b knockdown; in *Tg(hsp70l:mesp-ba^{myc})* embryos 15 min after heat shock, the expression of *myoD* and *myf5* in the lateral paraxial mesoderm was downregulated, and the expression of *meox1* was upregulated (Fig. 3A-C; supplementary material Fig. S5). The rapid changes in mRNA levels occurred similarly in all somites, independent of their maturation state, and did not affect the
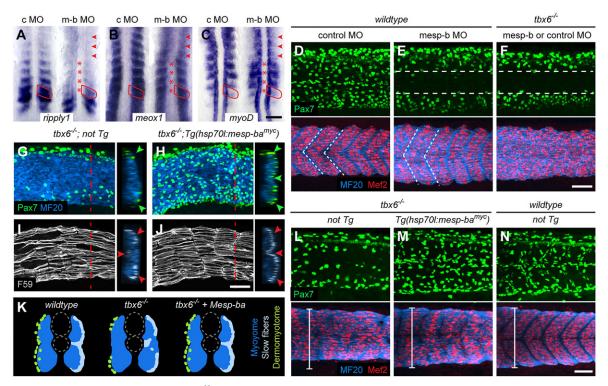
Fig. 2. Mesp-b knockdown recapitulates and Mesp-ba^{Myc} expression rescues dermomyotome phenotype in *tbx6* mutants. (A-F) Control and Mesp-b ATG MO-injected embryos at the 12-somite (A-C) and 24-h (D-F) stage. (A) *ripply1*, (B) *meox1* and (C) *myoD* mRNA expression. Red asterisks indicate most recently formed somites; SI is outlined; red arrowheads indicate downregulation of all three genes in maturing somites. (D-F) Immunolabeling showing dermomyotome (Pax7, green) and corresponding myotome (MF20, blue; Mef2, red). Mesp-b morphants phenocopy *tbx6* mutant dermomyotome but form somites similar to wild type; Mesp-b knockdown has no effect in *tbx6* mutants. Dashed lines indicate central dermomyotome domain (top) and somite boundaries (bottom). (G-J,L-N) Non-transgenic and *Tg(hsp70l:mesp-ba^{myc})* *tbx6* mutants heat-shocked at the 12-somite stage. (G-J) Transgenic embryos show increase in Pax7$^+$ dermomyotome cells (G,H) and rescued patterning of slow muscle fibers (F59, gray) within the myotome (MF20, blue) (I,J). (K) Schematic illustrating rescue of *tbx6* mutant phenotypes by transient Mesp-ba^{Myc} expression. (L-N) Transgenics develop larger myotomes (brackets), and show partially rescued myotome boundaries, similar to wild type. Scale bars: 100 μm in C; 50 μm in F,J,N.

developing slow muscle fibers in the medial paraxial mesoderm. This suggests that specific effects on myogenic marker genes are immediately downstream of Mesp-b.

pax3 is expressed in myogenic progenitors in future anterior and posterior somite domains before being restricted to the developing dermomyotome (Groves et al., 2005). We could not detect differences in *pax3* mRNA levels between transgenic embryos and non-transgenic siblings at this stage (Fig. 3D), indicating that Mesp-ba does not directly regulate *pax3* expression, and that the total population of dermomyotome and fast muscle fibers was not altered by ubiquitous Mesp-ba expression.

Six hours post heat shock (24-somite stage), the dorsal-to-ventral extent of *myoD* expression was reduced in *Tg(hsp70l:mesp-ba^{myc})* embryos, whereas *meox1* was still upregulated, particularly in somites formed during transgene expression (Fig. 3E,F). Smaller myotomes in *Tg(hsp70l:mesp-ba^{myc})* embryos showed a deficit specifically in differentiated fast muscle fibers, which expressed myosin heavy chain protein (MF20) and low levels of Mef2 in non-transgenic siblings (Fig. 3G,H). By contrast, slow muscle fiber differentiation was comparable in transgenic and non-transgenic embryos.

Nine hours post heat shock (24-h stage), *Tg(hsp70l:mesp-ba^{myc})* embryos had an increased number of mature, Pax7$^+$ dermomyotome cells (Fig. 3I,J), which spatially correlated with the decrease in *myoD* expression 6 h after heat shock (Fig. 3E). However, myotome sizes were similar in transgenic and non-transgenic embryos at this stage. The recovery of fast muscle indicates that dermomyotome-derived myogenesis is not disrupted in *Tg(hsp70l:mesp-ba^{myc})* embryos and compensates for the initial muscle deficit.

Together, these results show that transient ubiquitous expression of Mesp-ba causes immediate changes in dermomyotome and myotome marker gene expression, which correlate with an inhibition of fast muscle development and an increase in the number of Pax7$^+$ dermomyotome cells.

Ripply1 is necessary and sufficient for the elimination of Tbx6 protein

To determine whether Ripply1 negatively regulates Tbx6 protein, as seen in the context of somite formation in mouse (Takahashi et al., 2010), we knocked down Ripply1 function using MOs. As previously shown (Kawamura et al., 2005), knockdown of Ripply1 caused a loss of somite boundary formation, similar to the segmentation phenotype seen in *tbx6* mutants.

In Ripply1 morphants during segmentation stages, *tbx6* mRNA and protein were present at high levels throughout the paraxial mesoderm (Fig. 4A,B). Reflecting the expression of Tbx6 in Ripply1 morphants, both *mesp-b* paralogs were expressed in one to three stripes in the presomitic mesoderm (PSM), similar to their expression in control embryos, but remained upregulated in the anterior paraxial mesoderm (Fig. 4C,D). These expression patterns are consistent with previous work (Kawamura et al., 2005), and suggest that Ripply1 restricts the expression of Tbx6 to the pre-somitic mesoderm, where spatially restricted co-regulators further confine *mesp-b* expression to the future anterior half-somite.
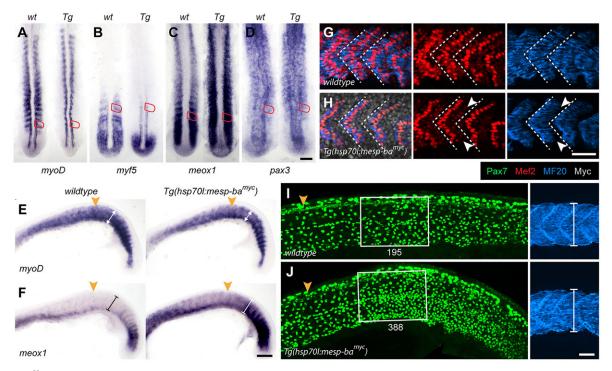
Fig. 3. Mesp-ba^Myc inhibits fast fiber differentiation and promotes dermomyotome development. *Tg(hsp70l:mesp-ba^myc)* embryos and wild-type siblings 1 h (A-D), 6 h (24-somite stage) (E-H) and 9 h (24-h stage) (I,J) after the end of heat shock. (A-D) Transgenic embryos show downregulation of *myoD* (A) and *myf5* mRNA (B) in the lateral paraxial mesoderm, and upregulation of *meox1* (C), but no difference in *pax3* (D). Most recently formed somite SI is outlined. (E,F) *myoD* expression shows smaller myotomes (E, brackets) in somites formed after heat shock (orange arrowhead); *meox1* mRNA is upregulated throughout those somites (F, brackets). (G,H) In transgenic embryos (Myc+, gray), the number of slow muscle nuclei (Mef2, bright red) is similar to wild type, but fast fiber nuclei (Mef2, faint red) and myosin heavy chain protein (MF20, blue) are reduced (arrowheads). (I,J) Immunolabeling shows increase in Pax7+ dermomyotome cells (green) in *Tg(hsp70l:mesp-ba^myc)* embryos (number indicated); boxed areas show underlying myotomes (MF20, blue) on the right. Orange arrowheads mark last somite formed before heat shock. Scale bars: 100 μm in D,F; 50 μm in H,J.

Ubiquitous expression of Ripply1 in *Tg(hsp70l:ripply1^myc)* embryos eliminated Tbx6 protein in the pre-somitic mesoderm, while only slightly reducing *tbx6* mRNA (Fig. 4E,F), thus supporting a role for Ripply1 in regulating Tbx6 at the protein level. Consistent with a lack of Tbx6 protein, *mesp-ba* expression was downregulated and *myoD* mRNA was upregulated in transgenic embryos (Fig. 4G; supplementary material Fig. S6A). To independently test whether Ripply1 promotes degradation of Tbx6 protein we injected either control or Ripply1 MOs into *Tg(hsp70l:tbx6^myc)^v8* embryos, heat-shocked for 30 min during segmentation stages and fixed 15 min post heat shock (supplementary material Fig. S6B). In Ripply1 morphants, endogenous Tbx6 protein was present in paraxial mesoderm cells along the entire anterior-posterior axis; transgene expression led to additional Tbx6 protein in the notochord and surface ectoderm. Control MO-injected embryos also show high levels of Tbx6 expression in the notochord and surface ectoderm, but not in the paraxial mesoderm. Thus, Tbx6 protein is immediately removed specifically from the paraxial mesoderm in a Ripply1-dependent manner.

Mesp-ba induces negative feedback

Ubiquitous Mesp-ba expression in *Tg(hsp70l:mesp-ba^myc)* embryos increased *ripply1* mRNA levels in wild type and induced *ripply1* expression in *tbx6* mutants (Fig. 4H,I), suggesting that Tbx6 regulation of *ripply1* is also mediated by Mesp-b in zebrafish, as in mouse (Morimoto et al., 2007).

In *Tg(hsp70l:mesp-ba^myc)* embryos after heat shock, Mesp-ba^Myc protein levels remained high throughout the paraxial mesoderm for several hours after transgene induction (Fig. 3H). However,

mesp-ba mRNA was highly upregulated only in the intermediate mesoderm and neural tube of transgenic embryos, whereas mRNA levels in the paraxial mesoderm were reduced, including expression from the endogenous *mesp-ba* gene (Fig. 4J). Conversely, knockdown of Mesp-b function caused an increase in *mesp-b* mRNA expression (Fig. 4K).

Together, these data suggest that Mesp-b downregulates its own mRNA, possibly via induction of Ripply1 and consequent Tbx6 protein degradation.

Ripply1 function is required for maturation and fast muscle fiber differentiation

In contrast to transient upregulation of Mesp-ba in *Tg(hsp70l: mesp-ba^myc)* embryos, knockdown of Ripply1 causes continuously high levels of *mesp-b* expression (Fig. 3 and Fig. 4C,D) (Kawamura et al., 2005). We hypothesized that this would amplify the myogenic phenotypes seen in transgenic embryos and further increase the number of Pax7+ dermomyotome cells.

Ripply1 knockdown did not have an effect in *tbx6* mutants (supplementary material Fig. S7A), indicating that Ripply1 acts mainly through elimination of Tbx6 protein. Similar to *Tg(hsp70l: mesp-ba^myc)* embryos after heat shock, Ripply1 knockdown reduced expression of *myoD* in the lateral paraxial mesoderm (Fig. 3A; supplementary material Fig. S7B). Surprisingly, knockdown of Ripply1, although causing high levels of Tbx6, *mesp-b* and *meox1*, resulted in downregulation of *pax3* mRNA (Fig. 5A,B; supplementary material Fig. S7C). In wild type, *pax3* is expressed at the beginning of both dermomyotome and fast muscle development (Groves et al., 2005); thus, a lack of *pax3*
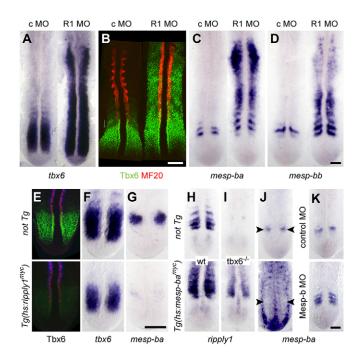
Fig. 4. Ripply1 terminates *tbx6* and *mesp-b* expression in the pre-somitic mesoderm. (A-D) Control and Ripply1 MO-injected embryos at the 12-somite stage labeled for *tbx6* (A, mRNA; B, protein), and *mesp-ba* (C) and *mesp-bb* mRNA (D). All markers are upregulated in the absence of Ripply1. MF20 (B, red) labels slow muscle progenitors. (E-G) *Tg(hsp70l:ripply1myc)* embryos and non-transgenic sibling 0.5 h (E) and 1 h (F,G) post heat shock. Transgenics lose expression of Tbx6 protein (E) and *mesp-ba* mRNA (G), *tbx6* mRNA is only slightly reduced (F). (H-J) *Tg(hsp70l:mesp-bamyc)* embryos and non-transgenic siblings 1 h post heat shock. Ubiquitous expression of Mesp-ba leads to upregulation of *ripply1* mRNA in wild type and *tbx6* mutants (H,I). *mesp-ba* mRNA is not ubiquitously upregulated after *Tg(hsp70l:mesp-bamyc)*: levels are low in the paraxial mesoderm, endogenous *mesp-ba* expression (arrowheads) is downregulated (J). (K) Control and Mesp-b MO-injected embryos labeled for *mesp-ba* mRNA. Scale bars: 100 µm.

expression indicates a general inhibition of myogenesis in the lateral paraxial mesoderm.

We did not observe Pax7$^+$ dermomyotome cells or differentiated fast muscle fibers in the presence of Tbx6 protein (Fig. 5C,D; supplementary material Fig. S7D). The elimination of Tbx6 protein in Ripply1 morphants took about 8 h, compared with 30 min in the presence of Ripply1, but similarly occurred in an anterior-to-posterior progression. At the 22-somite stage, Tbx6 protein had disappeared from the anterior trunk of Ripply1 morphants, but was still present in the posterior half of the embryo (Fig. 5C). At the same time, the first mature Pax7$^+$ dermomyotome cells appeared in the anterior trunk (Fig. 5D). In the first ~6 somites, which develop independently of Tbx6 function (Windner et al., 2012), *tbx6*, *mesp-b* and *meox1* expression remained elevated for a longer period, and Pax7 expression was further delayed (Fig. 4A,C,D; data not shown).

At the 24-h stage, ectopic *tbx6* was restricted to the most recently formed somites in the tail, whereas *pax3* and *pax7* were highly upregulated throughout the anterior and posterior trunk in Ripply1 morphants (Fig. 5E-G). Immunolabeling confirmed a dramatic increase in the number of Pax7$^+$ dermomyotome cells, most prominent in the central domain of the trunk (Fig. 5H,I). Fast muscle differentiation was completely inhibited prior to upregulation of Pax7, whereas slow muscle fibers differentiated but remained in a position adjacent to the notochord (Fig. 5J,K; supplementary

material Fig. S7E). This indicates that knockdown of Ripply1 leads to the induction of dermomyotome development throughout the lateral paraxial mesoderm, at the expense of fast muscle formation, and raises the possibility that, in the absence of Ripply1, fast muscle fibers are exclusively derived from Pax7$^+$ dermomyotome cells.

Combined, these results suggest that continuous expression of Tbx6 and/or Tbx6-dependent genes inhibits myogenesis in the lateral paraxial mesoderm. The Ripply1-dependent elimination of Tbx6 protein prior to somite formation restricts dermomyotome development to anterior half-somites, which facilitates fast muscle differentiation in posterior half-somites.

DISCUSSION
We have explored a gene regulatory network in zebrafish that regulates some of the earliest steps in embryonic myogenesis. Our results significantly extend previous work on the interactions between *tbx6*, *mesp-b* and *ripply1*, and introduce novel roles for Mesp-b and Ripply1 in the specification and maturation of dermomyotome and myotome, respectively. We propose a model that explains how the readout of genes associated with segmentation leads to the spatially restricted specification of myogenic progenitors within the somites, and to the temporal coordination of myogenesis with the formation of somite boundaries (Fig. 6).

Molecular interactions between *tbx6*, *mesp-b* and *ripply1*
Our data suggest that Tbx6 directly regulates the expression of both *mesp-b* paralogs *in vivo* (see also Kawamura et al., 2008; Cutty et al., 2012). Binding of Tbx6 to the *mesp-b* promoter and the functional relevance of this interaction have been demonstrated in other vertebrate models, including medaka (Terasaki et al., 2006), *Xenopus* (Tazumi et al., 2008) and mouse (Yasuhiko et al., 2006, 2008), suggesting that this interaction is conserved. Mesp genes are expressed in one to three precise bands prior to somite boundary formation (Saga et al., 1997; Sawada et al., 2000). The restriction of *mesp-b* expression to the anterior half of future somites in mouse depends on the spatially restricted overlap of Tbx6 with active Notch signaling (Saga, 2012). Oscillating Notch activity is a fundamental component of the segmentation clock, also in zebrafish (Oates et al., 2012). Whether the restricted expression of zebrafish *mesp-b* represents a direct output of the segmentation clock is not known.

We provide the first evidence that Tbx6 directly regulates the expression of the transcriptional co-repressor *ripply1*. We also demonstrate that Mesp-ba can induce *ripply1* in the absence of Tbx6, which is in accordance with studies showing direct activation of the orthologous mouse *Ripply2* by Mesp2 (Morimoto et al., 2007). Further, we show that Mesp-b is not required for the expression of *ripply1* in the anterior PSM but is required for the maintenance of *ripply1* expression in the somites. Together, these results indicate that Tbx6 induces *ripply1* expression in the pre-somitic mesoderm, whereas Mesp-b promotes continued expression within the somites. Our data do not indicate whether Mesp-ba regulation of *ripply1* in zebrafish is direct or indirect.

We show that Ripply1 is necessary and sufficient for the elimination of Tbx6 protein prior to somite formation in zebrafish. Whether this is by ubiquitin-dependent protein degradation, as it is in mouse, remains to be determined (Oginuma et al., 2008; Takahashi et al., 2010). Ripply proteins recruit Groucho/TLE co-repressors to repress Tbx-mediated transcription of *mesp* genes in zebrafish and *Xenopus* (Kondow et al., 2007; Kawamura et al., 2008). Thus, Ripply family members might suppress Tbx6 function in multiple ways. The Ripply1-dependent inhibition of Tbx6 function restricts the activation
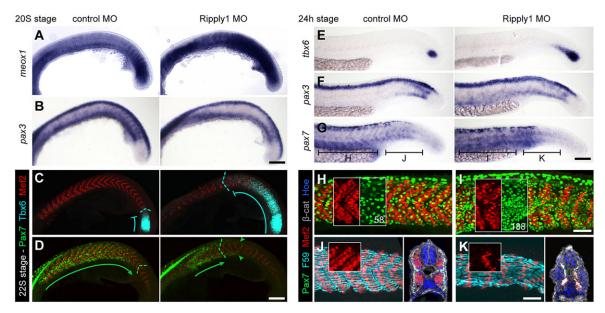
Fig. 5. Ripply1 knockdown inhibits fast muscle development, dermomyotome maturation is delayed. Control and Ripply1 morphants at the 20-somite (A,B), 22-somite (C,D) and 24-h stage (E-K). (A,B) Ripply1 morphants show upregulation of *meox1* (A) and downregulation of *pax3* (B) mRNA. (C,D) In control embryos, Tbx6 is restricted to pre-somitic mesoderm, Pax7$^+$ dermomyotome cells populate somites 1-18; in Ripply1 morphants, Tbx6 protein is expanded into the posterior trunk, Pax7$^+$ cells are restricted to somites ~7-14 (D). The Pax7 and Tbx6 expression domains (green and cyan lines, respectively) do not overlap; the dorsal and ventral domains of the trunk develop faster than the central domain (arrowheads). (E-G) At 24 h, *tbx6* mRNA expression is only slightly expanded in Ripply1 morphants (E); *pax3* (F) and *pax7* (G) are highly upregulated. (H,I) Immunolabeling shows an increase in Pax7$^+$ dermomyotome cells in Ripply1 morphants. Boxes separately show Mef2$^+$ (red) and Pax7$^+$ nuclei (green, number indicated). (J,K) In wild type, slow muscle fibers (F59, cyan) are found lateral to fast fibers; Ripply1 morphants completely lack fast fibers (red, on cross-sections in J,K), slow fibers lie adjacent to the axial structures. β-catenin labels cell membranes, Hoechst all nuclei. Axis levels of images in H-K are indicated in G. Scale bars: 100 µm in B,D,G; 50 µm in I,K.

of *mesp-b* genes to the pre-somitic mesoderm; additional negative feedback might be involved in the rapid downregulation of *mesp* mRNA before somite boundary formation.

Mesp-b regulates dermomyotome development and myotome patterning

The Tbx6-dependent expression of *mesp-b* genes precedes the upregulation of the dermomyotome markers *pax3/7* in space and time (Fig. 6A,B). Pax3 is expressed throughout the lateral paraxial mesoderm immediately before somite boundary formation. The developing dermomyotome cells in the anterior half of the lateral somite maintain *pax3*, and subsequently express *pax7*, whereas downregulation of pax3 and activation of *myoD* and *myf5* leads to differentiation of fast muscle fibers (Groves et al., 2005; Devoto et al., 2006). Signaling molecules, including Fgf8, regulate the onset of *myoD* expression, but not its spatial restriction to the posterior half of the lateral somite (Groves et al., 2005). We propose that *mesp-b* genes promote dermomyotome development in the anterior half-somite.

tbx6 mutants, which do not express *mesp-b*, upregulate *myoD* in the lateral paraxial mesoderm without spatial restriction (van Eeden et al., 1996). This phenotype correlates with an increase in fast fiber nuclei and a decrease in Pax3$^+$/Pax7$^+$ dermomyotome cells, whereas the total number of myogenic nuclei remains the same, thus suggesting ectopic development of fast muscle at the expense of dermomyotome cells in *tbx6* mutants (Windner et al., 2012). Here, we show that *mesp-b* is not expressed in the dorsal and ventral periphery of the somite, and that *mesp-b* morphants recapitulate the specific loss of central dermomyotome seen in *tbx6* mutants, whereas Mesp-ba overexpression rescues the dermomyotome and myotome phenotypes in *tbx6* mutants. Thus, *mesp-b* gene expression regulates the establishment of the central

dermomyotome cell population downstream of Tbx6. Normal development of peripheral dermomyotome in *tbx6* mutants and Mesp-b morphants suggests different genetic regulation; whether peripheral dermomyotome cells have a different developmental origin remains to be determined.

We demonstrate that Mesp-b expression immediately upregulates the dermomyotome marker *meox1* and inhibits the expression of *myoD* and *myf5*, specifically in the lateral paraxial mesoderm. Genome-wide transcriptional analysis after Mesp1 induction in mouse cell culture has shown that Mesp1 rapidly activates and represses specific sets of target genes, and thus acts as a key regulatory switch during cardiovascular progenitor cell specification (Bondue et al., 2008). Similarly, we suggest that *mesp-b* genes in the paraxial mesoderm act as an intrinsic determinant for the establishment of the central dermomyotome cell population by activating dermomyotome genes, while at the same time repressing genes promoting the alternative cell fate, the fast myotome. Thus, ubiquitous expression of *mesp-b* in Ripply1 morphants leads to widespread dermomyotome development and completely inhibits fast muscle differentiation throughout the paraxial mesoderm. However, we show that *mesp-b* genes do not immediately promote *pax3/7* expression, which is consistent with *in vivo* analyses placing *pax* genes downstream of *meox1* gene function (Mankoo et al., 2003), but could also indicate that *mesp-b* and *pax3* genes synergistically regulate dermomyotome development.

Taken together, our data provide an explanation for the initial pattern of dermomyotome and fast muscle progenitors in the zebrafish somites. Whether the Mesp-dependent regulation of myogenesis is conserved in vertebrates remains to be determined. In mouse, it has been suggested that *mesp* genes regulate the ability of cells to contribute to the dermomyotome by affecting the process of epithelialization (Takahashi et al., 2005). Thus, it is
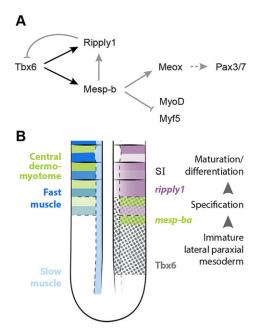
Fig. 6. Gene network regulating specification and maturation of myogenic progenitors. (A) Proposed interactions between Tbx6, Mesp-b and Ripply1 leading to specification of central dermomyotome progenitors (*meox1*, *pax3/7* expression) and inhibition of myogenic differentiation (*myoD* and *myf5* expression). Black lines represent direct interactions shown in this study; gray lines indicate missing evidence for direct interaction; dashed line indicates direct or indirect interactions. (B) Spatial and temporal correlation between development of different myogenic cell populations (left side) and expression of Tbx6 protein and *mesp-ba* and *ripply1* mRNA (right side). Tbx6 expression characterizes immature cells in the lateral paraxial mesoderm prior to boundary formation (SI); Mesp-b specifies central dermomyotome cells in the future anterior half-somite, Ripply1 promotes maturation of dermomyotome and differentiation fast muscle progenitors.

possible that Mesp target genes effect dermomyotome development in various ways, including morphological changes in the paraxial mesoderm.

Slow muscle fibers are induced by Hedgehog signaling from notochord and ventral neural tube in the medial paraxial mesoderm and start differentiating prior to and independent of Tbx6 expression (van Eeden et al., 1996; Blagden et al., 1997; Du et al., 1997; Windner et al., 2012). Slow fibers are not displaced to the lateral somite surface in Ripply1 morphants, in which dermomyotome maturation is delayed, nor in *tbx6* mutants, in which dermomyotome differentiates prematurely into fast muscle. Thus, the translocation of slow fibers depends on properly timed specification and maturation of dermomyotome and fast fibers in the lateral somite. Although Mesp-b expression can rescue the slow fiber phenotype in *tbx6* mutants, it remains to be determined whether Mesp-b affects myotome patterning directly by regulating muscle progenitor translocation, and/or indirectly by regulating the balance between dermomyotome and fast muscle, which could subsequently shape the somite.

Mesp-b and somite boundary formation

Mesp gene expression reliably marks the position of future somite boundaries in the anterior pre-somitic mesoderm and is implicated in regulating somite boundary formation via induction of components of the Eph signaling pathway (Nakajima et al., 2006; Dahmann et al., 2011). The role of Mesp genes in segmentation is well established in mouse (Saga, 2012); however, only *mesp-1/mesp-2* double knockout leads to the complete loss of

morphological somite boundaries (Oginuma et al., 2008). We find that irregular somite boundaries persist following knockdown of *mesp-b* in zebrafish (see also Akiyama et al., 2014). We suggest that this might reflect a functional redundancy with *mesp-a* genes, which show similar expression patterns and regulation (Sawada et al., 2000; Cutty et al., 2012). Conversely, transient ubiquitous expression of Mesp-ba is insufficient to completely rescue somite formation in *tbx6* mutants, suggesting that segmental/polarized expression of *mesp* and/or other genes downstream of Tbx6 is required for proper somite boundary formation. The identification of Mesp-b target genes will provide insights into whether the different cellular processes attributed to *mesp* genes result from one or multiple pathways of gene activation.

Ripply1 promotes maturation of myogenic progenitors

Ripply1 is expressed in the future anterior and posterior half-somites prior to boundary formation and negatively regulates Tbx6 and *mesp-b* expression (Kawamura et al., 2005; this study). Our results show that Tbx6 protein has to be removed for the expression of *pax3/7* and *myoD* in the lateral paraxial mesoderm, indicating that Tbx6 and/or Tbx6-dependent genes inhibit maturation of myogenic cells. Downstream of Tbx6, Mesp-ba promotes dermomyotome development but does not immediately promote *pax3* expression, raising the possibility that *mesp* genes are among the Tbx6 targets that have to be downregulated for dermomyotome maturation. A similar mechanism has been shown in cell culture studies, in which transient expression of Mesp1 promotes the differentiation of cardiac progenitors, whereas continuous expression inhibits it (Bondue et al., 2008). We suggest that, by promoting Tbx6 protein degradation, Ripply1 triggers maturation of myogenic progenitors in the lateral paraxial mesoderm (Fig. 6).

In the context of somite boundary formation, the region in the anterior paraxial mesoderm where pre-somitic mesoderm markers are downregulated and somite-specific markers are induced has been termed the determination front/wavefront (Dubrulle et al., 2001). The molecular changes occurring at the front determine the position of future somite boundaries, and include arrest of the segmentation clock and induction of stable expression of genes characterizing future anterior and posterior half-somites (Holley, 2007; Aulehla and Pourquié, 2010; Oates et al., 2012). The appropriate axial position of the front is influenced by signaling gradients: Fgf and Wnt signaling from the tailbud and retinoic acid signaling from the maturing somites (Aulehla and Pourquié, 2010). In zebrafish, *ripply1* expression is directly promoted by retinoic acid (Moreno et al., 2008), and thus constitutes a direct readout of the determination front. We propose that the Ripply1-dependent degradation of Tbx6 protein participates in the developmental switch occurring at the determination front, triggering the morphological segmentation of the paraxial mesoderm, as well as the formation of dermomyotome and myotome.

Although the major components of the determination front are conserved across different vertebrate models, some of the molecular mechanisms seem to be species-specific (Moreno et al., 2008). Future work will determine whether the inhibition of Tbx6 is a conserved feature of the front and coordinates the onset of myogenesis with somite boundary formation also in other vertebrates.

MATERIALS AND METHODS
Animals
All animal experiments were undertaken according to protocols approved by the Wesleyan University Animal Care and Use Committee, assurance number A3956-01.

Zebrafish, transgenesis, heat shock

We used wild-type zebrafish (*Danio rerio*) and the *ti1* or *te314a* allele of *fss/ tbx6* mutants, each of which behaves as a null (Nikaido et al., 2002). We detected no differences between wild type and heterozygote *tbx6* mutants, and for readability refer to heterozygous embryos as wild type. We used the *Tg(hsp70l:tbx6^myc)^v8* line and generated stable transgenic lines, using full-length *mesp-ba*, *mesp-bb* (Cutty et al., 2012) and *ripply1* (Kawamura et al., 2005) cDNAs, and gateway cloning as previously described (Kwan et al., 2007; Villefranc et al., 2007; Windner et al., 2012). All plasmids were verified by sequencing. Heat shocks were performed as previously described (Windner et al., 2012), for 1 h at 37°C, unless stated otherwise. Transgenics were identified using anti-cMyc antibody labeling or PCR genotyping. Embryos were cared for using standard procedures (Westerfield, 1995).

Generation of anti-Tbx6 monoclonal antibody

8 µg of a Tbx$_{6327-545}$ peptide fused to GST was injected into Balb/c mice; sera were screened via ELISA. Each antiserum with a positive signal was further tested for tissue-specific binding in 15-somite stage wild-type and *tbx6* mutant embryos. Hybridoma cell lines were produced from one mouse; antibodies were purified from the supernatants. The antibody with highest signal-to-noise ratio was used for experiments (Clone: A83-1, IgG1).

Morpholino (MO) knockdown and RT-PCR

MOs (GeneTools) were resuspended to obtain 1 µM stock solutions, and diluted 1:5 before co-injection with p53 MO into the yolk at the 1-cell stage. MO sequences are included in supplementary material Table S3.

For RT-PCR, embryos were injected with Mesp-ba or Mesp-bb splice-blocking and p53 MOs; total RNA was extracted from ~50 embryos at bud stage with TRIzol reagent (Life Technologies), with additional RQ1 DNase I treatment (Promega). cDNA was produced using GoScript Reverse Transcriptase (Promega), primers used for PCR are shown in supplementary material Table S3.

In situ hybridization, immunocytochemistry, imaging

Fixations, whole-mount RNA *in situ* hybridization and immunohistochemistry were carried out as previously described (Barresi et al., 2000; Patterson et al., 2010; Windner et al., 2012). Antibodies and RNA probes used are listed in supplementary material Table S3. Images of immunolabeled whole-mounts were taken with a Zeiss LSM510 confocal microscope, and confocal *z*-stacks were flattened. Cryostat cross-sections and *in situ* hybridization samples were imaged on a Zeiss Axioplan compound microscope, and on a Leica stereomicroscope, respectively. Embryos at 20-somite (19-h) stage and older are shown in lateral view, dorsal up, anterior left; younger stages are in dorsal view, anterior up.

ChIP-seq

Tg(hsp70l:tbx6^myc) and wild-type embryos were heat-shocked at the 10-somite stage, and fixed 1 h later. ChIP for 2000 embryos per replicate, using 10 µg goat anti-Myc tag antibody (Abcam, ab9132), was carried out as in Wardle et al. (2006), with the exception that purified immunoprecipitated DNA was directly prepared for Illumina sequencing using the TruSeq DNA sample prep kit, with DNA adapters diluted 1:100. Paired-end sequencing of ChIP and their matched input samples were sequenced on an Illumina HiSeq. Duplicate ChIP-seq experiments were performed for *Tg(hsp70l: tbx6^myc)* and a single control experiment in wild-type embryos.

To define Tbx6^Myc binding sites, paired end sequence fragments with unique outer coordinates were mapped to the danRer7 genome build using Bowtie (Langmead et al., 2009) with the following parameters: -5 3 -3 30 –n 3 –y –k 2 –m 2 –best. Peaks were called for each ChIP sample relative to their paired input sample using MACS (Zhang et al., 2008) with the following parameters: –gsize 1.3e+9 –tsize 67 -mfold 8 –pval 5e-10 for Tbx6^Myc ChIP samples and –mfold 4 for the wild-type Myc tag control ChIP. Reported peaks are present in both *Tg(hsp70l:tbx6^myc)* ChIP-seq experiment and absent in the wild-type control. Motif analysis was performed using Weeder v1.4.2 with default parameters (Pavesi et al., 2006), except that both strands were processed; Tbx6^Myc binding peaks which were significant in both experiments were used. All ChIP-seq data are stored in NCBI Gene Expression Omnibus under the accession number GSE57332.

T-box identification

For identification of potential T-boxes within genomic regions represented in Fig. 1F, a modified version of the Perl scripts in the TFBS suite was used (Lenhard and Wasserman, 2002) to identify matches to the position frequency matrix generated by Weeder v1.4.2 (see above).

Author contributions
S.E.W. and S.H.D. designed the study, S.E.W. carried out most experiments with help from C.M.F. R.A.D. assembled plasmids for transgenics, carried out ChIP-PCR and provided embryos for ChIP-seq. A.C.N. designed and carried out IP, library preparation for the ChIP-seq and computational analysis. G.V. created and validated the anti-Tbx6 monoclonal antibody. H.T. designed Mesp-b MOs and performed RT-PCR validation. A.C.O. directed anti-Tbx6 antibody production. F.C.W. directed ChIP-seq experiments and Mesp-b MO design/validation. A.C.O. and F.C.W. provided ideas and discussion throughout the study. S.E.W. and S.H.D. wrote the manuscript with contributions from all other authors.

Supplementary material
Supplementary material available online at
http://dev.biologists.org/lookup/suppl/doi:10.1242/dev.113431/-/DC1

References
Akiyama, R., Masuda, M., Tsuge, S., Bessho, Y. and Matsui, T. (2014). An anterior limit of FGF/Erk signal activity marks the earliest future somite boundary in zebrafish. *Development* **141**, 1104-1109.

Aulehla, A. and Pourquié, O. (2010). Signaling gradients during paraxial mesoderm development. *Cold Spring Harb. Perspect. Biol.* **2**, a000869.

Barresi, M. J., Stickney, H. L. and Devoto, S. H. (2000). The zebrafish slow-muscle-omitted gene product is required for Hedgehog signal transduction and the development of slow muscle identity. *Development* **127**, 2189-2199.

Blagden, C. S., Currie, P. D., Ingham, P. W. and Hughes, S. M. (1997). Notochord induction of zebrafish slow muscle mediated by Sonic hedgehog. *Genes Dev.* **11**, 2163-2175.

Bondue, A., Lapouge, G., Paulissen, C., Semeraro, C., Iacovino, M., Kyba, M. and Blanpain, C. (2008). Mesp1 acts as a master regulator of multipotent cardiovascular progenitor specification. *Cell Stem Cell* **3**, 69-84.

Brend, T. and Holley, S. A. (2009). Expression of the oscillating gene her1 is directly regulated by hairy/enhancer of split, T-box, and suppressor of Hairless proteins in the zebrafish segmentation clock. *Dev. Dyn.* **238**, 2745-2759.

Buckingham, M. and Relaix, F. (2007). The role of Pax genes in the development of tissues and organs: Pax3 and Pax7 regulate muscle progenitor cell functions. *Annu. Rev. Cell Dev. Biol.* **23**, 645-673.

Buckingham, M. and Rigby, P. W. J. (2014). Gene regulatory networks and transcriptional mechanisms that control myogenesis. *Dev. Cell* **28**, 225-238.

Buckingham, M. and Vincent, S. D. (2009). Distinct and dynamic myogenic populations in the vertebrate embryo. *Curr. Opin. Genet. Dev.* **19**, 444-453.

Cutty, S. J., Fior, R., Henriques, P. M., Saúde, L. and Wardle, F. C. (2012). Identification and expression analysis of two novel members of the Mesp family in zebrafish. *Int. J. Dev. Biol.* **56**, 285-294.

Dahmann, C., Oates, A. C. and Brand, M. (2011). Boundary formation and maintenance in tissue development. *Nat. Rev. Genet.* **12**, 43-55.

Devoto, S. H., Stoiber, W., Hammond, C. L., Steinbacher, P., Haslett, J. R., Barresi, M. J. F., Patterson, S. E., Adiarte, E. G. and Hughes, S. M. (2006).

Generality of vertebrate developmental patterns: evidence for a dermomyotome in fish. *Evol. Dev.* **8**, 101-110.

Du, S. J., Devoto, S. H., Westerfield, M. and Moon, R. T. (1997). Positive and negative regulation of muscle cell identity by members of the hedgehog and TGF-beta gene families. *J. Cell Biol.* **139**, 145-156.

Dubrulle, J., McGrew, M. J. and Pourquié, O. (2001). FGF signaling controls somite boundary position and regulates segmentation clock control of spatiotemporal Hox gene activation. *Cell* **106**, 219-232.

Garnett, A. T., Han, T. M., Gilchrist, M. J., Smith, J. C., Eisen, M. B., Wardle, F. C. and Amacher, S. L. (2009). Identification of direct T-box target genes in the developing zebrafish mesoderm. *Development* **136**, 749-760.

Groves, J. A., Hammond, C. L. and Hughes, S. M. (2005). Fgf8 drives myogenic progression of a novel lateral fast muscle fibre population in zebrafish. *Development* **132**, 4211-4222.

Hammond, C. L., Hinits, Y., Osborn, D. P. S., Minchin, J. E. N., Tettamanti, G. and Hughes, S. M. (2007). Signals and myogenic regulatory factors restrict pax3 and pax7 expression to dermomyotome-like tissue in zebrafish. *Dev. Biol.* **302**, 504-521.

Holley, S. A. (2007). The genetics and embryology of zebrafish metamerism. *Dev. Dyn.* **236**, 1422-1449.

Hollway, G. E., Bryson-Richardson, R. J., Berger, S., Cole, N. J., Hall, T. E. and Currie, P. D. (2007). Whole-somite rotation generates muscle progenitor cell compartments in the developing zebrafish embryo. *Dev. Cell* **12**, 207-219.

Kawamura, A., Koshida, S., Hijikata, H., Ohbayashi, A., Kondoh, H. and Takada, S. (2005). Groucho-associated transcriptional repressor required for proper transition from the presomitic mesoderm to somites. *Dev. Cell* **9**, 735-744.

Kawamura, A., Koshida, S. and Takada, S. (2008). Activator-to-repressor conversion of T-box transcription factors by the Ripply family of Groucho/TLE-associated mediators. *Mol. Cell. Biol.* **28**, 3236-3244.

Kispert, A. and Hermann, B. G. (1993). The Brachyury gene encodes a novel DNA binding protein. *EMBO J.* **12**, 4898-4899.

Kondow, A., Hitachi, K., Okabayashi, K., Hayashi, N. and Asashima, M. (2007). Bowline mediates association of the transcriptional corepressor XGrg-4 with Tbx6 during somitogenesis in Xenopus. *Biochem. Biophys. Res. Commun.* **359**, 959-964.

Kusakabe, R. and Kuratani, S. (2005). Evolution and developmental patterning of the vertebrate skeletal muscles: perspectives from the lamprey. *Dev. Dyn.* **234**, 824-834.

Kwan, K. M., Fujimoto, E., Grabher, C., Mangum, B. D., Hardy, M. E., Campbell, D. S., Parant, J. M., Yost, H. J., Kanki, J. P. and Chien, C.-B. (2007). The Tol2kit: a multisite gateway-based construction kit for Tol2 transposon transgenesis constructs. *Dev. Dyn.* **236**, 3088-3099.

Langmead, B., Trapnell, C., Pop, M. and Salzberg, S. L. (2009). Ultrafast and memory-efficient alignment of short DNA sequences to the human genome. *Genome Biol.* **10**, R25.

Lenhard, B. and Wasserman, W. W. (2002). TFBS: computational framework for transcription factor binding site analysis. *Bioinformatics* **18**, 1135-1136.

Mankoo, B. S., Skuntz, S., Harrigan, I., Grigorieva, E., Candia, A., Wright, C. V. E., Arnheiter, H. and Pachnis, V. (2003). The concerted action of Meox homeobox genes is required upstream of genetic pathways essential for the formation, patterning and differentiation of somites. *Development* **130**, 4655-4664.

Moreno, T. A., Jappelli, R., Izpisua Belmonte, J. C. and Kintner, C. (2008). Retinoic acid regulation of the Mesp-Ripply feedback loop during vertebrate segmental patterning. *Dev. Biol.* **315**, 317-330.

Morimoto, M., Sasaki, N., Oginuma, M., Kiso, M., Igarashi, K., Aizaki, K.-i., Kanno, J. and Saga, Y. (2007). The negative regulation of Mesp2 by mouse Ripply2 is required to establish the rostro-caudal patterning within a somite. *Development* **134**, 1561-1569.

Nakajima, Y., Morimoto, M., Takahashi, Y., Koseki, H. and Saga, Y. (2006). Identification of Epha4 enhancer required for segmental expression and the regulation by Mesp2. *Development* **133**, 2517-2525.

Nikaido, M., Kawakami, A., Sawada, A., Furutani-Seiki, M., Takeda, H. and Araki, K. (2002). Tbx24, encoding a T-box protein, is mutated in the zebrafish somite-segmentation mutant fused somites. *Nat. Genet.* **31**, 195-199.

Oates, A. C., Rohde, L. A. and Ho, R. K. (2005). Generation of segment polarity in the paraxial mesoderm of the zebrafish through a T-box-dependent inductive event. *Dev. Biol.* **283**, 204-214.

Oates, A. C., Morelli, L. G. and Ares, S. (2012). Patterning embryos with oscillations: structure, function and dynamics of the vertebrate segmentation clock. *Development* **139**, 625-639.

Oginuma, M., Hirata, T. and Saga, Y. (2008). Identification of presomitic mesoderm (PSM)-specific Mesp1 enhancer and generation of a PSM-specific Mesp1/Mesp2-null mouse using BAC-based rescue technology. *Mech. Dev.* **125**, 432-440.

Patterson, S. E., Bird, N. C. and Devoto, S. H. (2010). BMP regulation of myogenesis in zebrafish. *Dev. Dyn.* **239**, 806-817.

Pavesi, G., Mereghetti, P., Zambelli, F., Stefani, M., Mauri, G. and Pesole, G. (2006). MoD Tools: regulatory motif discovery in nucleotide sequences from co-regulated or homologous genes. *Nucleic Acids Res.* **34**, W566-W570.

Pourquié, O. (2011). Vertebrate segmentation: from cyclic gene networks to scoliosis. *Cell* **145**, 650-663.

Saga, Y. (2012). The mechanism of somite formation in mice. *Curr. Opin. Genet. Dev.* **22**, 331-338.

Saga, Y., Hata, N., Koseki, H. and Taketo, M. M. (1997). Mesp2: a novel mouse gene expressed in the presegmented mesoderm and essential for segmentation initiation. *Genes Dev.* **11**, 1827-1839.

Sawada, A., Fritz, A., Jiang, Y. J., Yamamoto, A., Yamasu, K., Kuroiwa, A., Saga, Y. and Takeda, H. (2000). Zebrafish Mesp family genes, mesp-a and mesp-b are segmentally expressed in the presomitic mesoderm, and Mesp-b confers the anterior identity to the developing somites. *Development* **127**, 1691-1702.

Stellabotte, F., Dobbs-McAuliffe, B., Fernandez, D. A., Feng, X. and Devoto, S. H. (2007). Dynamic somite cell rearrangements lead to distinct waves of myotome growth. *Development* **134**, 1253-1257.

Stellabotte, F. and Devoto, S. H. (2007). The teleost dermomyotome. *Dev. Dyn.* **236**, 2432-2443.

Takahashi, Y., Hiraoka, S., Kitajima, S., Inoue, T., Kanno, J. and Saga, Y. (2005). Differential contributions of Mesp1 and Mesp2 to the epithelialization and rostro-caudal patterning of somites. *Development* **132**, 787-796.

Takahashi, J., Ohbayashi, A., Oginuma, M., Saito, D., Mochizuki, A., Saga, Y. and Takada, S. (2010). Analysis of Ripply1/2-deficient mouse embryos reveals a mechanism underlying the rostro-caudal patterning within a somite. *Dev. Biol.* **342**, 134-145.

Tazumi, S., Yabe, S., Yokoyama, J., Aihara, Y. and Uchiyama, H. (2008). pMesogenin1 and 2 function directly downstream of Xtbx6 in Xenopus somitogenesis and myogenesis. *Dev. Dyn.* **237**, 3749-3761.

Terasaki, H., Murakami, R., Yasuhiko, Y., Shin, I. T., Kohara, Y., Saga, Y. and Takeda, H. (2006). Transgenic analysis of the medaka mesp-b enhancer in somitogenesis. *Dev. Growth Differ.* **48**, 153-168.

van Eeden, F. J., Granato, M., Schach, U., Brand, M., Furutani-Seiki, M., Haffter, P., Hammerschmidt, M., Heisenberg, C. P., Jiang, Y. J., Kane, D. A. et al. (1996). Mutations affecting somite formation and patterning in the zebrafish, Danio rerio. *Development* **123**, 153-164.

Villefranc, J. A., Amigo, J. and Lawson, N. D. (2007). Gateway compatible vectors for analysis of gene function in the zebrafish. *Dev. Dyn.* **236**, 3077-3087.

Wardle, F. C., Odom, D. T., Bell, G. W., Yuan, B., Danford, T. W., Wiellette, E. L., Herbolsheimer, E., Sive, H. L., Young, R. A. and Smith, J. C. (2006). Zebrafish promoter microarrays identify actively transcribed embryonic genes. *Genome Biol.* **7**, R71.

Westerfield, M. (1995). *The Zebrafish Book*, 3rd ed. Eugene, Oregon, University of Oregon Press.

Windner, S. E., Bird, N. C., Patterson, S. E., Doris, R. A. and Devoto, S. H. (2012). Fss/Tbx6 is required for central dermomyotome cell fate in zebrafish. *Biol. Open* **1**, 806-814.

Yasuhiko, Y., Haraguchi, S., Kitajima, S., Takahashi, Y., Kanno, J. and Saga, Y. (2006). Tbx6-mediated Notch signaling controls somite-specific Mesp2 expression. *Proc. Natl. Acad. Sci. USA* **103**, 3651-3656.

Yasuhiko, Y., Kitajima, S., Takahashi, Y., Oginuma, M., Kagiwada, H., Kanno, J. and Saga, Y. (2008). Functional importance of evolutionarily conserved Tbx6 binding sites in the presomitic mesoderm-specific enhancer of Mesp2. *Development* **135**, 3511-3519.

Zhang, Y., Liu, T., Meyer, C. A., Eeckhoute, J., Johnson, D. S., Bernstein, B. E., Nusbaum, C., Myers, R. M., Brown, M., Li, W. et al. (2008). Model-based analysis of ChIP-Seq (MACS). *Genome Biol.* **9**, R137.

DEVELOPMENT